An Integrated Controller For Stabilizing An Inverted Pendulum: LQR And Fuzzy Logic Control With Observer-Based State Estimation

Thi-Van-Anh Nguyen* and Ngoc-Hiep Tran

School of Electrical and Electronic Engineering, Hanoi University of Science and Technology

*Corresponding author. E-mail: anh.nguyenthivan1@hust.edu.vn

Received: Jun. 08, 2023; Accepted: Jul. 31, 2023

This paper addresses the challenging control problem of stabilizing an inverted pendulum on a cart. The inherent nonlinearity, instability, and underactuation of the system pose significant difficulties in achieving simultaneous pendulum stabilization and cart movement. To overcome these challenges, we propose an integrated approach that combines Linear Quadratic Regulator (LQR) and fuzzy logic control methods. This integrated control strategy effectively stabilizes the pendulum and controls the cart's position. Notably, the integrated control outperforms the LQR control in terms of convergence speed. Furthermore, we explore the use of observers for state estimation, specifically the high-order integral-chain differentiator and the extended state observer, to accurately estimate pendulum angular velocity. Simulation results, along with detailed discussions, are presented to validate the accuracy and effectiveness of the proposed control methods and observers.

Keywords: Inverted pendulum; Fuzzy logic control; Linear quadratic regulator; Extended state observer; High-order integral-chain differentiator

http://dx.doi.org/10.6180/jase.202405_27(5).0006

1. Introduction

The inverted pendulum is a fascinating area of research that has garnered significant attention from many scholars [1, 2]. This is a classic example of a challenging control problem in the field of control systems engineering due to its inherent nonlinearity, instability, and underactuation. It has practical applications in a variety of fields, including human balance modeling [3] and the design of self-balancing two-wheeled electric vehicles [4]. In this paper, we focus on studying the control technique for the inverted pendulum on a cart. The system is described as Fig. 1 where a cart moves along a track and the goal is to keep the pendulum balanced in a vertical position while the cart moves.

There are multiple challenges associated with controlling an inverted pendulum. Firstly, the system's inherent nonlinearity and instability imply that even minor variations in initial conditions or external disturbances can cause the pendulum to collapse. Secondly, the system is underactuated, meaning that there is only one control input (the horizontal force applied to the cart) but two degrees of freedom (the position of the cart and the angle of the pendulum). This makes designing a control system that can stabilize the pendulum while simultaneously moving the cart a difficult task. There are several control methods that can be used to stabilize an inverted pendulum system, including: proportional-integral-derivative (PID) control [5], model predictive control (MPC) [6], sliding mode control (SMC) [7], linear quadratic regulator (LQR) [8], fuzzy logic control [9] ... LQR, a simple control method that requires a detailed understanding of the system dynamics, has a fast response that enables quick stabilization of the pendulum and prevents it from falling over. Fuzzy logic control [10] is a nonlinear control method so that it can handle the nonlinear dynamics of an inverted pendulum system. It is also a robust control method that can handle uncertainties and

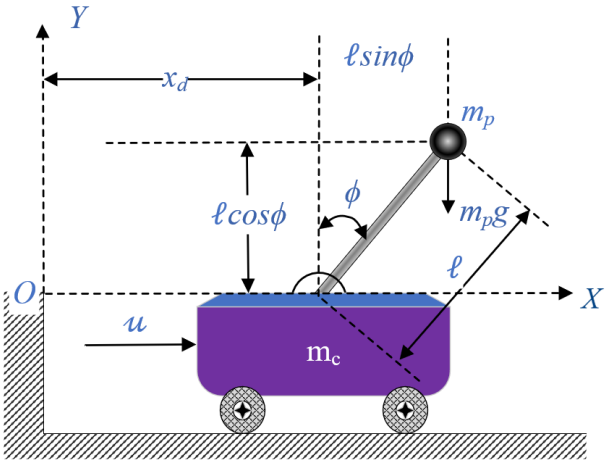

Fig. 1. Model of inverted pendulum on a cart.

disturbances in the system. This allows the controller to adjust to changes in the system dynamics and maintain stable control of the system. Therefore, we combine both of these control techniques. By combining these two controllers, not only did we aim to achieve pendulum stability, but we also sought to enhance performance. The integration of these controllers resulted in faster stabilization and setup times for the pendulum, thus improving overall system performance.

Building on the strengths of both control methods, the combination of LQR and Fuzzy Logic Control (FLC) has been a subject of research and development. In a recent paper [11], the inverted pendulum system is represented using a Takagi-Sugeno (TS) fuzzy model, converting the nonlinear system into multiple linear subsystems. Each of these subsystems is then controlled using LQR controllers. The control signals from these LQR controllers are combined using a parallel distribution compensator (PDC) to control the entire system. Another approach, presented in references [12], involves combining Mamdani fuzzy control with LQR. In this method, the LQR controller's value is computed first and then used to design the Linear Fusion Function (LFF). However, determining the appropriate language variables for the control signals in this approach can be challenging and relies heavily on the designer's experience. Even though the systems studied in the aforementioned articles differ from the inverted pendulum on the cart, the combination of control methods demonstrated its efficacy and feasibility, suggesting its potential applicability to the inverted pendulum system on the cart as well. To improve upon these methods, we propose a novel combination in which the LQR and Fuzzy controllers are independently calculated, and the final control signal is synthesized based on the outputs of both controllers. This new approach aims to harness the benefits of each method effectively and achieve superior control performance for the inverted pendulum system.

The dynamics of the system can be characterized by the cart's position and velocity, the pendulum's angle and angular velocity, and the applied force. However, in practical applications, direct measurement of all these states, particularly the angular velocity of the pendulum, may not be feasible. To address this limitation, observers [13] are employed to estimate the unmeasured states. By providing accurate estimations, these observers enhance the performance of the control system. In this study, we utilize the high-order integral-chain differentiator and extended state observer as the chosen observers. Through a comparison of the results obtained using both observers for pendulum angle velocity estimation and stability control, the high-order integral-chain differentiator demonstrated superior performance compared to the extended state observer in terms of error estimation and peak overshoot.

This article presents several significant contributions in the field of inverted pendulum control:

- Designing an integrated control approach by combining Linear Quadratic Regulator (LQR) and Takagi-Sugeno (T-S) fuzzy control methods. This integration enhances control performance and facilitates faster convergence of control signals.
- The high-order integral-chain differentiator and extended state observer are utilized to accurately estimate the angular velocity of the pendulum. This allows for precise state estimation with small error.
- Demonstrating the efficacy of the composite controller on both the pendulum and cart position. The results indicate that the proposed control approach achieves successful stabilization and control of the inverted pendulum on a cart system.
- Validation of the obtained results through simulation results of the inverted pendulum on a cart, confirming the practical applicability and effectiveness of the proposed control methods.

2. Inverted pendulum modeling

In the model of an inverted pendulum on a cart shown in Fig. 1, the mass of the pendulum is denoted by m_p (kg), the mass of the cart is denoted by m_c (kg), the length of the connecting rod is denoted by ℓ (m) and the rotation angle of the pendulum from the Y-axis is denoted by ϕ. The force affecting the cart in the X-axis is denoted by u and g represents the acceleration due to gravity. The coordinates

of the pendulum are defined as ($\tilde{x}$,$\tilde{y}$), where x_d represents the distance traveled by the cart.

$$\tilde{x} = x_d + \ell sin\phi,\ \tilde{y} = \ell cos\phi \tag{1}$$

With the potential energy is $E_P = m_p g\ell cos\phi$ and the kinetic energy is $E_K = \frac{1}{2}m_c\dot{x}_d^2 + \frac{1}{2}m_p(\dot{\tilde{x}}^2 + \dot{\tilde{y}}^2)$, the Lagrange equation can be derived as:

$$L = E_K - E_P = \frac{1}{2}(m_c + m_p)\dot{x}_d^2 + \frac{1}{2}m_p\ell^2\dot{\phi}^2 + m_p\ell\dot{\phi}\dot{x}_d cos\phi - m_p g\ell cos\phi. \tag{2}$$

To construct a model of an inverted pendulum on a cart, the Euler-Lagrange equation is required:

$$\frac{\mathrm{d}}{\mathrm{d}t}(\frac{\delta L}{\delta \dot{x}_d}) - \frac{\delta L}{\delta x_d} = u,\ \frac{\mathrm{d}}{\mathrm{d}t}(\frac{\delta L}{\delta \dot{\phi}}) - \frac{\delta L}{\delta \phi} = 0. \tag{3}$$

Using the Euler-Lagrange equation as above, the kinematic equation is derived:

$$\begin{cases} (m_c + m_p)\,\ddot{x}_d + m_p\ell\ddot{\phi}\cos\phi - m_p\ell\dot{\phi}^2\sin\phi = u, \\ \ell\ddot{\phi} + \ddot{x}_d\cos\phi - g\sin\phi = 0. \end{cases} \tag{4}$$

The angle of the pendulum and cart distance dynamics are obtained by merge and transform those set of Eq. (4):

$$\begin{cases} \ddot{\phi} = \frac{(m_c+m_p)g\sin\phi - m_p\ell\phi^2\sin\phi\cos\phi - u\cos\phi}{\ell\left[m_p(1-\cos^2\phi)+m_c\right]}, \\ \ddot{x}_d = \frac{-m_p g\sin\phi\cos\phi + m_p\ell\phi^2\sin\phi + u}{m_p(1-\cos^2\phi)+m_c}. \end{cases} \tag{5}$$

Let the state variables as $x = [\,x_d\ \dot{x}_d\ \phi\ \dot{\phi}\,]^\top$ and the Eq. (5) can be expressed as:

$$\dot{x} = \mathcal{A}x + \mathcal{B}u, \tag{6}$$

where

$$\mathcal{A} = \begin{bmatrix} 0 & 1 & 0 & 0 \\ 0 & 0 & \frac{-m_p g\sin\phi\cos\phi}{\phi\left[m_p(1-\cos^2\phi)+m_c\right]} & \frac{m_p\ell\dot{\phi}\sin\phi}{m_p(1-\cos^2\phi)+m_c} \\ 0 & 0 & 0 & 1 \\ 0 & 0 & \frac{(m_c+m_p)g\sin\phi}{\phi\ell\left[m_p(1-\cos^2\phi)+m_c\right]} & \frac{-m_p\ell\dot{\phi}\sin\phi\cos\phi}{e\left[m_p(1-\cos^2\phi)+m_c\right]} \end{bmatrix},$$

$$\mathcal{B} = \begin{bmatrix} 0 \\ \frac{1}{m_p(1-\cos^2\phi)+m_c} \\ 0 \\ \frac{-\cos\phi}{\ell\left[m_p(1-\cos^2\phi)+m_c\right]} \end{bmatrix} \tag{7}$$

Once the system of kinematic equations for the pendulum on the cart has been established, the subsequent step involves designing controllers to achieve stable control of the pendulum.

3. Control design for enhanced system performance

In this section, we will discuss a control design approach aimed at improving the performance of a stable controller for an inverted pendulum on a cart system. Specifically, two control techniques will be combined: Linear Quadratic Regulator (LQR) and Takagi-Sugeno (T-S) fuzzy control. The proposed fuzzy controller will be designed to enhance the stability of the pendulum angle, which is the main objective of controlling the inverted pendulum on the cart. In order to calculate the control signal using LQR, the state variables of the system need to be defined as $x = [\,x_d\ \dot{x}_d\ \phi\ \dot{\phi}\,]^\top$. However, since the fuzzy logic controller is only concerned with stabilizing the pendulum angle, we can simplify the system model by using a reduced state variable vector, denoted by $\bar{x} = [\phi\ \dot{\phi}\,]^\top$. x_{ref}, ϕ_{ref} denote the reference of cart position and pendulum angle, respectively. The total control signal is presented as:

$$u = \bar{u} + \tilde{u}. \tag{8}$$

where $\tilde{u}$, $\bar{u}$ is LQR and T-S control signal, respectively.

3.1. Linear Quadratic Regulator

While the inverted pendulum system is nonlinear, it is possible to use linear control techniques such as LQR (Linear Quadratic Regulator) to stabilize it. LQR is a control strategy designed for linear systems, but it can be applied to nonlinear systems like the inverted pendulum by linearizing the system dynamics around an operating point. This involves approximating the nonlinear system by a linear one within a small region around the equilibrium point. In the context of linearization around the equilibrium point and employing the LQR controller for nonlinear systems, findings from the article [14] have provided valuable insights. The study showcased that within the active region surrounding the equilibrium point, the approximated linear model exhibits a response closely resembling that of the original nonlinear model. Moreover, the LQR controller effectively governs the system within this active region, demonstrating its capability in controlling the nonlinear dynamics of the system. These results affirm the feasibility and efficiency of using LQR-based control techniques for stabilizing nonlinear systems within their operational regions. Given a system in state-space form:

$$\dot{x} = \mathcal{A}x(t) + \mathcal{B}\tilde{u}(t) \tag{9}$$

where $\tilde{u}$ is the LQR control signal. A finite-horizon cost function is define as:

$$Q = \int_0^\infty (x^\top Mx + \tilde{u}^\top N\tilde{u})dt,\ M = M^\top \succeq 0,\ N = N^\top \succ 0. \tag{10}$$

The purpose is finding the optimal cost-to-go function $Q^*(x)$ which satisfy this equation:

$$0 = \min_{\tilde{u}}[x^\top M x + \tilde{u}^\top N \tilde{u} + \frac{\partial Q^*}{\partial x}(\mathcal{A}x + \mathcal{B}\tilde{u})],\ \forall x. \quad (11)$$

The optimal cost-to-go function is quadratic and chosen as $Q^*(x) = x^\top \lambda x,\ \lambda = \lambda^\top \succeq 0$. The gradient function is $\frac{\partial Q^*}{\partial x} = 2x^\top \lambda$. Finding the solution of $\frac{\partial}{\partial \tilde{u}} = 2\tilde{u}^\top N + 2x^\top \lambda \mathcal{B} = 0$ is equivalent to solving Eq. (11), in which all the terms are convex and quadratic. The control signal $\tilde{u}$ is derived as:

$$\tilde{u} = -N^{-1}\mathcal{B}^\top \lambda x = -\mathcal{K}x. \quad (12)$$

Substituting this into Eq. (11) and simplifying, we obtain $0 = x^\top[M - \lambda\mathcal{B}N^{-1}\mathcal{B}^\top\lambda + \lambda\mathcal{A} + \mathcal{A}^\top\lambda]x$. Since this condition must hold for all x, this means:

$$M - \lambda\mathcal{B}N^{-1}\mathcal{B}^\top\lambda + \lambda\mathcal{A} + \mathcal{A}^\top\lambda = 0. \quad (13)$$

This function can be solved by calling $\mathcal{K} = lqr(\mathcal{A}, \mathcal{B}, M, N)$ in MATLAB's Simulink. With the control signal in Eq. (12), the closed-loop can be expressed as $\dot{x} = (\mathcal{A} - \mathcal{B}\mathcal{K})x$. Choose the Lyapunov function:

$$V(x) = x^\top \lambda x. \quad (14)$$

Take the derivative with respect to time of Eq. (14):

$$\begin{aligned}\dot{V}(x) = \frac{\partial V}{\partial x}\frac{dx}{dt} &= 2x^\top\lambda(\mathcal{A} - \mathcal{B}\mathcal{K})x \\ &= x^\top[\lambda(\mathcal{A} - \mathcal{B}\mathcal{K}) + (\mathcal{A} - \mathcal{B}\mathcal{K})^\top\lambda]x.\end{aligned} \quad (15)$$

From Eq. (13) and $\mathcal{K} = N^{-1}\mathcal{B}^\top\lambda$ in Eq. (12):

$$\begin{aligned}&\lambda\mathcal{A} - \lambda\mathcal{B}\mathcal{K} + \mathcal{A}^\top\lambda - \mathcal{K}^\top\mathcal{B}^\top\lambda + M = -\mathcal{K}^\top\mathcal{B}^\top\lambda \\ \Longleftrightarrow &\lambda(\mathcal{A} - \mathcal{B}\mathcal{K}) + (\mathcal{A} - \mathcal{B}\mathcal{K})^\top\lambda = -\mathcal{K}^\top N N^{-1}\mathcal{B}^\top\lambda - M \\ &= -\mathcal{K}^\top N\mathcal{K} - M\end{aligned} \quad (16)$$

We have $N \succ 0$ and $M \succeq 0$ then $-\mathcal{K}^\top N\mathcal{K} - M < 0 \Rightarrow \lambda(\mathcal{A} - \mathcal{B}\mathcal{K}) + (\mathcal{A} - \mathcal{B}\mathcal{K})^\top\lambda < 0$. The derivative $\dot{V}(x) < 0$ means the system is asymptotically stable with the control signal $\tilde{u} = -\mathcal{K}x$.

3.2. Pendulum stablization with Takagi-Sugeno Fuzzy model

Takagi-Sugeno models (T-S models) can effectively represent many nonlinear dynamics systems. There are two main approaches to construct a T-S model: identification based on input-output data or utilizing existing nonlinear equations. In this paper, the latter approach is adopted. The T-S model is formed by combining multiple linear subsystem models, where each subsystem corresponds to an IF-THEN rule that captures the local linear input/output relationship.

$$\begin{cases} \dot{\bar{x}}(t) = \mathcal{A}_m(z)\bar{x}(t) + \mathcal{B}_m(z)\bar{u}(t), \quad m = 1, 2, \dots 2^q, \\ y(t) = C_m\bar{x}(t), \end{cases} \quad (17)$$

where q is the number of premise variables and 2^q denote the number of model rules, m is the m^{th} rule, z is premise variable. The membership functions of corresponding premise variables z are defined as $w_m(z) = \prod_{i=1}^{q} h_i{}^{\eta}(z_i)$, $1 \le m \le 2^q, \eta \in \{0, 1\}$, h_i is the grade of membership function. Therefore,

$$\dot{\bar{x}}(t) = \sum_{m=1}^{2^q} w_m(z)\left\{\mathcal{A}_m(z)\bar{x}(t) + \mathcal{B}_m(z)\bar{u}(t)\right\}. \quad (18)$$

Next, the parallel distributed compensation (PDC) fuzzy controller for a subsystem is designed as $\bar{u}(t) = -\boldsymbol{F}_m\bar{x}(t)$, $m = 1, 2, \cdots 2^q$. And the overall fuzzy controller is obtained:

$$\bar{u}(t) = -\sum_{m=1}^{2^q} w_m(z)\boldsymbol{F}_m\bar{x}(t), \quad (19)$$

where the feedback gain for m^{th} rule is $\boldsymbol{F}_m$. Combining Eq. (18) with Eq. (19), the equation describing the system is as follows:

$$\dot{\bar{x}}(t) = \sum_{m=1}^{2^q}\sum_{n=1}^{2^q} w_m(z)w_n(z)[\mathcal{A}_m(z) - \mathcal{B}_m(z)\boldsymbol{F}_n]\bar{x}(t). \quad (20)$$

Following the Theorem in [15], the closed-loop system is asymptotically stable if there exist a common positive definite matrix S and matrices H_n that satisfy the following inequalities.

$$\begin{cases} \mathcal{A}_m S - \mathcal{B}_m H_m + S\mathcal{A}_m^\top - H_m^\top\mathcal{B}_m^\top < 0, \\ \mathcal{A}_m S - \mathcal{B}_m H_n + S\mathcal{A}_m^\top - H_n^\top\mathcal{B}_m^\top \\ +\mathcal{A}_n S - \mathcal{B}_n H_m + S\mathcal{A}_n^\top - H_m^\top\mathcal{B}_n^\top < 0, \end{cases} \quad (21)$$

where $m, n \in \{1, 2, \cdots 2^q\}, m < n$. As a result, the control gains $\boldsymbol{F}_n$ of the PDC controller can be deduced $\boldsymbol{F}_n = H_n S^{-1}$. Proof: With Q being a positive definite matrix, the Lyapunov function is chosen as follows:

$$\mathcal{V}(\bar{x}) = \bar{x}^\top(t)Q\bar{x}(t). \quad (22)$$

Taking derivative of $\mathcal{V}(\bar{x})$ with respect to t:

$$\dot{\mathcal{V}}(\bar{x}) = \dot{\bar{x}}^\top(t)Q\bar{x}(t) + \bar{x}^\top(t)(\dot{Q}\bar{x}(t) + Q\dot{\bar{x}}(t)). \quad (23)$$

Substituting Eq. (20) into Eq. (23), we obtain:

$$\begin{aligned}\dot{\mathcal{V}}(\bar{x}) &= \sum_{m=1}^{2^q}\sum_{n=1}^{2^q} w_m(z)w_n(z)\bar{x}^\top(t) \\ &\left[(\mathcal{A}_m - \mathcal{B}_m F_n)^\top Q + Q(\mathcal{A}_m - \mathcal{B}_m F_n)\right]\bar{x}(t) \\ &= \sum_{m=1}^{2^q} w_m^2(z)\bar{x}^\top(t)[(\mathcal{A}_m - \mathcal{B}_m F_m)^\top Q \\ &+ Q(\mathcal{A}_m - \mathcal{B}_m F_m)]\bar{x}(t) + 2\sum_{m=1}^{2^q}\sum_{m<n}^{2^q} w_m(z)w_n(z)\bar{x}^\top(t) \\ &\times [\left(\frac{(\mathcal{A}_m - \mathcal{B}_m F_n) + (\mathcal{A}_n - \mathcal{B}_n F_m)}{2}\right)^\top Q \\ &+ Q\frac{(\mathcal{A}_m - \mathcal{B}_m F_n) + (\mathcal{A}_n - \mathcal{B}_n F_m)}{2}]\bar{x}(t).\end{aligned} \tag{24}$$

Therefore, $\dot{\mathcal{V}}(\bar{x}) < 0, \bar{x} \neq 0$ is equivalent to

$$\begin{cases} \mathcal{A}_m^\top Q + Q\mathcal{A}_m - F_m^\top \mathcal{B}_m^\top Q - Q\mathcal{B}_m F_m < 0, \\ \mathcal{A}_m^\top Q + Q\mathcal{A}_m - F_n^\top \mathcal{B}_m^\top Q - Q\mathcal{B}_m F_n \\ +\mathcal{A}_n^\top Q + Q\mathcal{A}_n - F_m^\top \mathcal{B}_n^\top Q - Q\mathcal{B}_n F_m < 0. \end{cases} \tag{25}$$

We define $S = Q^{-1}$ then multiply Eq. (25) with the term S on left and right:

$$\begin{cases} S\mathcal{A}_m^\top + \mathcal{A}_m S - SF_m^\top \mathcal{B}_m^\top - \mathcal{B}_m F_m S < 0, \\ S\mathcal{A}_m^\top + \mathcal{A}_m S - SF_n^\top \mathcal{B}_m^\top - \mathcal{B}_m F_n S \\ +S\mathcal{A}_n^\top + \mathcal{A}_n S - SF_m^\top \mathcal{B}_n^\top - \mathcal{B}_n F_m S < 0. \end{cases} \tag{26}$$

For $S \succ 0$ and set $H_n = F_n S$, therefore $F_n = H_n S^{-1}$. Substituting into the above inequality shows:

$$\begin{cases} S\mathcal{A}_m^\top + \mathcal{A}_m S - H_m^\top \mathcal{B}_m^\top - \mathcal{B}_m H_m < 0, \\ S\mathcal{A}_m^\top + \mathcal{A}_m S - H_n^\top \mathcal{B}_m^\top - \mathcal{B}_m H_n + S\mathcal{A}_n^\top + \mathcal{A}_n S - H_m^\top \mathcal{B}_n^\top \\ -\mathcal{B}_n H_m < 0. \end{cases} \tag{27}$$

This concludes the proof.

The aim of this study is to apply the theoretical principles of Takagi-Sugeno control. In this section, a comprehensive overview of the Takagi-Sugeno control theory is provided, encompassing its construction methods and model synthesis techniques. Additionally, a state model, represented by Eq. (6), is introduced to describe the kinematic of the inverted pendulum on a cart system. The primary objective is to leverage the theory of model reconstruction and formulate a T-S fuzzy model structure to effectively control the behavior of the inverted pendulum system. Let the premise variables as:

$$\begin{aligned} z_1 &= \frac{1}{\ell[m_p(1-cos^2\phi)+m_c]}, z_2 = \frac{sin\phi}{\phi}, \\ z_3 &= cos\phi, z_4 = \dot{\phi}sin\phi. \end{aligned} \tag{28}$$

Substituting the premise variables z, we get:

$$\begin{aligned} \mathcal{A}_{TS} &= \begin{bmatrix} 0 & 1 \\ (m_c+m_p)gz_1z_2 & -m_p\ell z_1 z_3 z_4 \end{bmatrix}, \\ \mathcal{B}_{TS} &= \begin{bmatrix} 0 \\ -z_1 z_3 \end{bmatrix}, \end{aligned} \tag{29}$$

where $\mathcal{A}_{TS} = \sum_{m=1}^{16} w_m(z)\mathcal{A}_m(z)$ and $\mathcal{B}_{TS} = \sum_{m=1}^{16} w_m(z)\mathcal{B}_m(z)$. The model of the inverted pendulum system will consist of four premise variables which will result in the creation of 16 fuzzy rules (2^4) to capture the system's behavior accurately. Each fuzzy rule will describe a specific relationship between the inputs and outputs, enabling comprehensive control of the inverted pendulum. Let us define:

$$h_i^0 = \frac{z_{imax} - z_i}{z_{imax} - z_{imin}}, \quad h_i^1 = 1 - h_i^0, \quad i = 1,2,3,4. \tag{30}$$

Then, some membership functions of the T-S fuzzy model are:

$$\begin{aligned} w_1 &= h_1^0 * h_2^0 * h_3^0 * h_4^0; & w_2 &= h_1^1 * h_2^0 * h_3^0 * h_4^0; \\ w_{15} &= h_1^0 * h_2^1 * h_3^1 * h_4^1; & w_{16} &= h_1^1 * h_2^1 * h_3^1 * h_4^1. \end{aligned} \tag{31}$$

In order to accomplish the objective of the original problem, an integrated controller will be formulated by combining the control signals of LQR and T-S, as discussed in this section. The combined control signal can be expressed as follows:

$$u = \bar{u} + \tilde{u} = -\sum_{m=1}^{16} w_m(z)F_m\bar{x}(t) - \mathcal{K}x(t). \tag{32}$$

By examining the stability of the system under the combined control signal in Eq. (32), we introduce the Lyapunov function as follows:

$$V_{cb} = V + \mathcal{V}. \tag{33}$$

Here, V is defined in Eq. (14), and $\mathcal{V}$ is defined in Eq. (22). It is evident that $V_{cb} > 0$. Calculating the time derivative of V_{cb}, we obtain:

$$\dot{V}_{cb} = \dot{V} + \dot{\mathcal{V}}. \tag{34}$$

The terms $\dot{V}$ and $\dot{\mathcal{V}}$ have been previously proven to be negative. As a result, $\dot{V}_{cb} < 0$, confirming the asymptotic stability of the system under the combined control u.

4. Estimation of pendulum angular velocity: observer design and analysis

Determining of pendulum angular velocity is crucial in control systems. However, directly measuring pendulum angular velocity poses significant challenges. Observers provide a suitable solution to overcome this limitation. In this paper, we propose two observers: the high-order integral-chain differentiator and the extended state observer. These observers enable accurate estimation of pendulum angle velocity, facilitating effective control of the system.

4.1. High-order integral-chain differentiator

Following the presentation of high-order integral-chain differentiator in [16, 17], its expression for the system below is shown as:

$$\begin{cases} \dot{x}_1 = x_2, \\ \dot{x}_2 = x_3, \\ \vdots \\ \dot{x}_{k-1} = x_k \\ \dot{x}_k = f + hu, \\ y = x_1. \end{cases} \Longrightarrow$$

$$\begin{cases} \dot{\hat{x}}_1 = \hat{x}_{2,} \\ \dot{\hat{x}}_2 = \hat{x}_{3,}, \\ \vdots \\ \dot{\hat{x}}_k = \hat{x}_{k+1}, \\ \dot{x}_{k+1} = -\frac{\alpha_1}{\varepsilon^{k+1}}(\hat{x}_1 - x_1) - \frac{\alpha_2}{\varepsilon^k}\hat{x}_2 - \cdots - \frac{\alpha_k}{\varepsilon^2}\hat{x}_k - \frac{\alpha_{k+1}}{\varepsilon}\hat{x}_{k+1}, \end{cases} \tag{35}$$

where f, h are nonlinear functions, $\hat{x}_1, \hat{x}_2, \hat{x}_3, ..., \hat{x}_h, \hat{x}_{h+1}$ are estimated values, x_1 is practical value, ε is chosen sufficiently small, $\alpha_1, \alpha_2, ...\alpha_{h+1}$ are positive constant such that

$$s^{h+1} + \alpha_{h+1}s^h + \cdots + \alpha_2 s + \alpha_1 = 0 \tag{36}$$

is Hurwitz. Hence, arcording to [16], it can be inferred that:

$$\lim_{\varepsilon \to 0} \hat{x}_i = x_i, \quad i = 1, 2, \cdots, h. \tag{37}$$

Using model derived from section 2 and observing state of the system as the angular velocity of pendulum, the observer is designed as follows:

$$\begin{cases} \dot{\hat{x}}_1 = \hat{x}_2, \\ \dot{\hat{x}}_2 = \hat{x}_3, \\ \dot{\hat{x}}_3 = -\frac{\alpha_1}{\varepsilon^3}(\hat{x}_1 - \phi) - \frac{\alpha_2}{\varepsilon^2}\hat{x}_2 - \frac{\alpha_3}{\varepsilon}\hat{x}_3, \end{cases} \tag{38}$$

where $\hat{x}_1$ is estimated angle $\hat{\phi}$ of the pendulum, $\hat{x}_2$ is estimated angular velocity $\dot{\hat{\phi}}$ of the pendulum.

4.2. Extended state observer

According to [18], by regarding f as an extended state x_{h+1}, the extended state observer for the below system is designed as:

$$\begin{cases} \dot{x}_1 = x_2, \\ \dot{x}_2 = x_3, \\ \vdots \\ \dot{x}_{h-1} = x_h, \\ \dot{x}_h = f + hu, \\ y = x_1. \end{cases} \Rightarrow \begin{cases} \dot{\hat{x}}_1 = \hat{x}_2 - \frac{\beta_1}{\varepsilon}(\hat{x}_1 - y), \\ \dot{\hat{x}}_2 = \hat{x}_3 - \frac{\beta_2}{\varepsilon^2}(\hat{x}_1 - y), \\ \vdots \\ \dot{\hat{x}}_{h-1} = \hat{x}_h - \frac{\beta_{h-1}}{\varepsilon^{h-1}}(\hat{x}_1 - y), \\ \dot{\hat{x}}_h = hu + \hat{x}_{h+1} - \frac{\beta_h}{\varepsilon^h}(\hat{x}_1 - y), \\ \dot{\hat{x}}_{h+1} = -\frac{\beta_{h+1}}{\varepsilon^{h+1}}(\hat{x}_1 - y). \end{cases} \tag{39}$$

where f, h are nonlinear functions. In this paper's control problem, the observer's input is ϕ and the variable that requires estimation is the angular velocity of the pendulum. Hence, the observer should be:

$$\begin{cases} \dot{\hat{x}}_1 = \hat{x}_2 - \frac{\beta_1}{\varepsilon}(\hat{x}_1 - \phi), \\ \dot{\hat{x}}_2 = bu + \hat{x}_3 - \frac{\beta_2}{\varepsilon^2}(\hat{x}_1 - \phi), \\ \dot{\hat{x}}_3 = -\frac{\beta_3}{\varepsilon^3}(\hat{x}_1 - \phi), \end{cases} \tag{40}$$

where $\hat{x}_1$, $\hat{x}_2$, $\hat{x}_3$ are the states of observer, ε>0, b is equal to $\frac{cos\phi}{\ell[m_p(1-cos^2\phi)+m_c]}$. β_1, β_2, β_3 are positive constants and polynomial $s^3 + \beta_1 s^2 + \beta_2 s + \beta_3$ is Hurwitz. It has:

$$\lim_{\varepsilon \to 0} \hat{x}_1 = x_1, \qquad \lim_{\varepsilon \to 0} \hat{x}_2 = x_2, \qquad \lim_{\varepsilon \to 0} \hat{x}_3 = f, \tag{41}$$

with $\hat{x}_1$ is estimated angle $\hat{\phi}$ of the pendulum, $\hat{x}_2$ is estimated angular velocity $\dot{\hat{\phi}}$ of the pendulum, f represent the disturbance in the system.

5. Simulation and result

In simulation, parameters of the pendulum and the cart are chosen as: $m_p = 0.2(kg), g = 9.8(m/s^2), m_c = 1(kg), \ell = 1(m)$. The initial conditions of state variables are $x_{d0} = 0\,(m), \dot{x}_{d0} = 0\,(m/s), \phi_0 = \frac{\pi}{9}\,(rad), \dot{\phi}_0 = 0\,(rad/s)$. With the determined parameters, z_{imax}, z_{imin} are fixed, see Table 1. Following the equations Eqs. (30) and (31), h_i^0, h_i^1 and w_m can be calculated, respectively. The coefficient of observers are chosen as: $\alpha_1 = 1$, $\alpha_2 = 3$, $\alpha_3 = 3$, $\beta_1 = 6$, $\beta_2 = 11$, $\beta_3 = 6$, $\varepsilon = 0.01$. Furthermore, MATLAB's Robust Control Toolbox help us in solving LMI problem to find out the feedback gain $\boldsymbol{F}_n$. Then, the control signal $\bar{u}$ is derived. By chosing M and N as follow: $M = \begin{bmatrix} 50 & 0 & 0 & 0 \\ 0 & 1 & 0 & 0 \\ 0 & 0 & 50 & 0 \\ 0 & 0 & 0 & 1 \end{bmatrix}$, $N = 1$, the gain $\mathcal{K}$ can be calculated as $\mathcal{K} = [\,-7.0711 \quad -8.6224 \quad -62.6499 \quad -19.2600\,]$. The simulation results of the pendulum system are presented through Fig. 2, depicting the pendulum angle and the angular velocity. To assess the effectiveness of the proposed controller, we conduct a comparative analysis with two other controllers: the LQR controller and the controller proposed in [11]. The controller in [11] also combines T-S fuzzy and LQR techniques, but it differs from the proposed controller as LQR is applied to the fuzzy subsystems in that case. Analyzing the pendulum angle, we observe that the proposed integrated controller achieves a settling time of 3.6227 seconds, which is faster than both LQR and the controller proposed in [11]. Similarly, for the angular velocity, the integrated controller demonstrates faster stabilization compared to these controllers. These findings provide substantial evidence supporting the superior convergence speed of the proposed integrated controller, see Table 2.

In Fig. 3 the blue lines represent the system states: cart position x_d and pendulum angle ϕ, when utilizing the high-order integral-chain differentiator. Conversely, the red lines

Table 1. Maximum and minimum values of the permise variables z.

i	1	2	3	4
z_{imax}	1	1	1	1
z_{imin}	0.8333	0.6366	6.1232×10^{-17}	-1

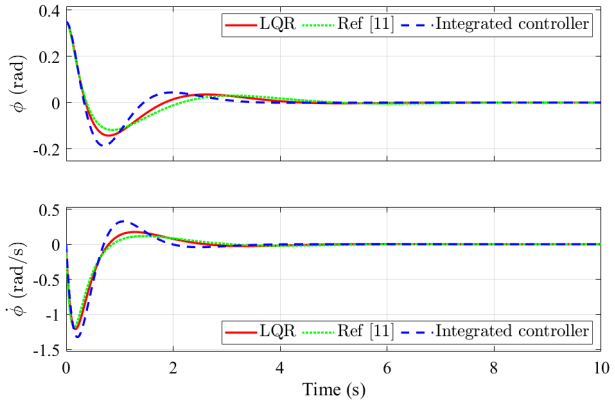

Fig. 2. The pendulum angle ϕ and angular velocity $\dot{\phi}$ when using LQR, controller in [11] and integrated controller.

depict the same state variables, but with the implementation of the extended state observer. These results are obtained under disturbance-free conditions. For both observers, the cart position stabilizes after 5.5 seconds and the pendulum angle takes more than 4 seconds to stabilize. The stabilization times of the state variables are similar when using the two observers. However, the extended state observer exhibits larger overshoots in the pendulum angle and cart position compared to the high-order integral-chain differentiator. Considering the limitations of the track, the high-order integral-chain differentiator outperforms when starting with a higher initial angle ϕ_0.

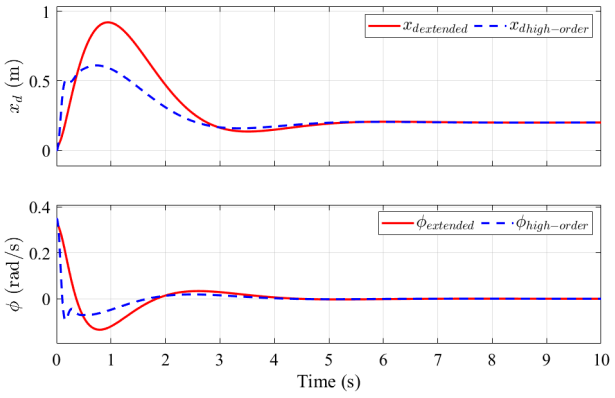

Fig. 3. The cart position x_d and pendulum angle ϕ in the absence of disturbance.

The estimated values in Fig. 4 correspond to the practical values. The extended state observer exhibits a faster response than the high-order integral-chain differentiator (0.08 seconds compared to 0.4 seconds). However, the extended state observer has a large peak at the start, resulting in a higher root mean square observed error than the high-order integral-chain differentiator. Table 3 provides the root mean square value as well as the maximum and minimum values of the errors of both observers. In Table 3, under disturbance-free conditions, the results indicate that the high-order integral-chain differentiator set outperforms in terms of estimation.

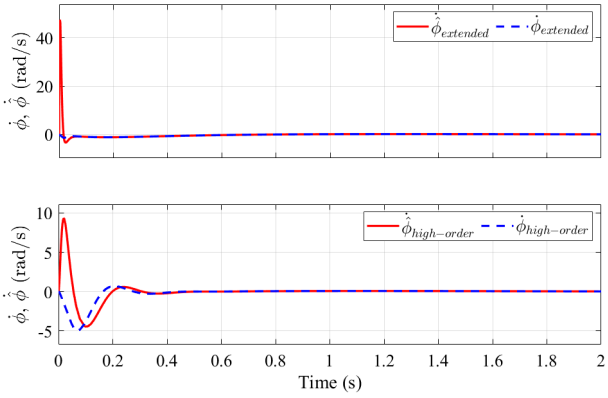

Fig. 4. Observer result of pendulum angular velocity $\dot{\phi}$ using both observers in the absence of disturbance.

In the presence of disturbance which is the white noise signal with noise power of 0.01 in Fig. 5, the state systems of the two observers are depicted in Fig. 6. Both observers achieve stable cart position after 5.5 seconds and the pendulum angle approach zero in approximately 4 seconds. Despite the presence of disturbance, the state variables exhibit oscillations around the equilibrium point and their stabilization times are not significantly affected. Similar to the case without disturbance, the extended state observer continues to exhibit larger overshoots in cart position x_d and pendulum angle ϕ compared to the high-order integral-chain differentiator.

Both observers demonstrate efficiency in handling the presence of disturbance. The time required for the estimated values to converge to the actual values does not show significant changes, see Fig. 7. However, in the presence of disturbance, the maximum and root mean square of estimated errors increase. In each case, the high-order integral-chain differentiator proves to be more suitable than the extended state observer.

Table 2. Performance comparison.

	Cart position (x_d)			Pendulum angle (ϕ)		
	Integrated	LQR	Ref [11]	Integrated	LQR	Ref [11]
Settling time (s)	3.6227	5.0289	8.0113	3.2138	4.0091	4.6497
Overshoot/ Undershoot	0.923 m	0.955 m	0.988 m	-0.187 rad	-0.142 rad	-0.118 rad

Table 3. Comparison between observed errors.

	Without disturbance	With disturbance
The root mean square error (high-order)	2.1564	2.163
The root mean square error (extended)	6.5751	7.0462
The maximum error (high-order)	10.89	10.89
The maximum error (extended)	47.64	47.83
The minimum error (high-order)	1.8080×10^{-9}	1.7755×10^{-9}
The minimum error (extended)	4.0585×10^{-7}	4.0585×10^{-7}

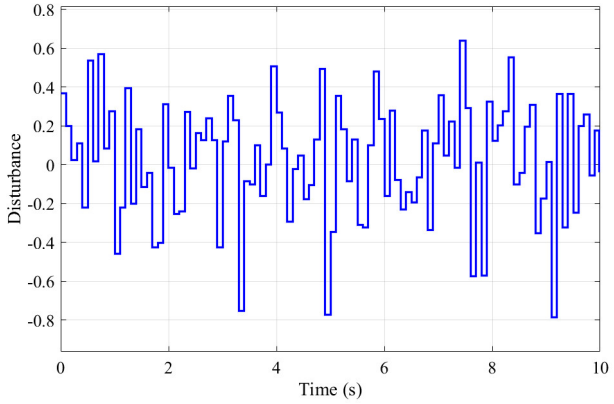

Fig. 5. Disturbance signal.

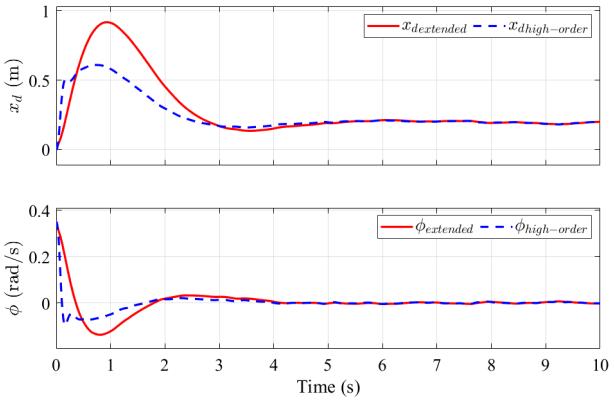

Fig. 6. The cart position x_d and pendulum angle ϕ in the presence of disturbance.

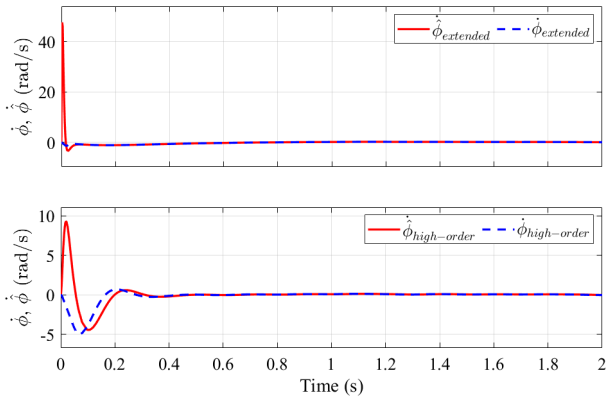

Fig. 7. Observer result of pendulum angular velocity $\dot{\phi}$ using both observers in the presence of disturbance.

6. Conclusion and discussion

In conclusion, this study successfully addressed the challenging control problem of the inverted pendulum on a cart. By integrating the Linear Quadratic Regulator (LQR) and Takagi-Sugeno (T-S) fuzzy control methods, the control performance was enhanced and faster convergence of controlled signals was achieved. The utilization of high-order integral-chain differentiator and extended state observer improved state estimation accuracy. The proposed composite controller demonstrated superior performance in stabilizing and controlling both the pendulum and cart position. Simulation results confirmed the effectiveness of the proposed control methods. Overall, this study contributes valuable insights and guidance for future research and practical applications in the field of control systems engineering.

The proposed control method faces challenges related to robustness in handling uncertainties in system dynamics, sensor measurements, and external disturbances. Moreover, the integration of multiple control techniques and observers may lead to increased complexity, hindering smooth implementation. To address these limitations, future work should focus on enhancing robustness by incorporating adaptive or robust control strategies, such as online parameter adaptation algorithms or real-time compen-

sation schemes. Additionally, efforts to streamline the control system's complexity can be pursued through advanced control synthesis techniques, model reduction methods, or optimization algorithms, ensuring efficient implementation and maintenance without compromising performance and stability.

References

[1] S. Zeghlache, M. Z. Ghellab, A. Djerioui, B. Bouderah, and M. F. Benkhoris, (2023) *"Adaptive fuzzy fast terminal sliding mode control for inverted pendulum-cart system with actuator faults"* **Mathematics and Computers in Simulation *210***: 207–234. DOI: https://doi.org/10.1016/j.matcom.2023.03.005.

[2] V.-A. Nguyen, D.-B. Pham, D.-T. Pham, N.-T. Bui, and Q.-T. Dao. "A Hybrid Energy Sliding Mode Controller for the Rotary Inverted Pendulum". In: *Advances in Engineering Research and Application: Proceedings of the International Conference on Engineering Research and Applications, ICERA 2022*. Springer. 2022, 34–41. DOI: https://doi.org/10.1007/978-3-031-22200-9_4.

[3] T. Zielinska, G. R. Rivera Coba, and W. Ge, (2021) *"Variable Inverted Pendulum Applied to Humanoid Motion Design"* **Robotica *39***(8): 1368–1389. DOI: 10.1017/S0263574720001228.

[4] S.-J. Huang, S.-S. Chen, and S.-C. Lin, (2019) *"Design and Motion Control of a Two-Wheel Inverted Pendulum Robot"* **International Journal of Mechanical and Mechatronics Engineering *13***(3): 194–201. DOI: doi.org/10.5281/zenodo.2643591.

[5] L. B. Prasad, B. Tyagi, and H. O. Gupta, (2014) *"Optimal control of nonlinear inverted pendulum system using PID controller and LQR: performance analysis without and with disturbance input"* **International Journal of Automation and Computing *11***: 661–670. DOI: https://doi.org/10.1007/s11633-014-0818-1.

[6] L. Messikh, E.-H. Guechi, and S. Blazic, (2021) *"Stabilization of the cart–inverted-pendulum system using state-feedback pole-independent MPC controllers"* **Sensors *22***(1): 243. DOI: https://doi.org/10.3390/s22010243.

[7] M. S. Mahmoud, R. A. Saleh, and A. Ma'arif, (2022) *"Stabilizing of inverted pendulum system using Robust sliding mode control"* **International Journal of Robotics and Control Systems *2***(2): 230–239. DOI: https://doi.org/10.3390/s22010243.

[8] A. Jose, C. Augustine, S. M. Malola, K. Chacko, et al., (2015) *"Performance study of PID controller and LQR technique for inverted pendulum"* **World Journal of Engineering and Technology *3***(02): 76. DOI: 10.4236/wjet.2015.32008.

[9] , (2017) *"Fuzzy-logic control of an inverted pendulum on a cart"* **Computers Electrical Engineering *61***: 31–47. DOI: https://doi.org/10.1016/j.compeleceng.2017.05.016.

[10] D.-B. Pham, D.-T. Pham, Q.-T. Dao, and V.-A. Nguyen. "Takagi-Sugeno fuzzy control for stabilizing nonlinear inverted pendulum". In: *Intelligent Systems and Networks: Selected Articles from ICISN 2022, Vietnam*. Springer, 2022, 333–341. DOI: https://doi.org/10.1007/978-981-19-3394-3_38.

[11] B. Sharma and B. Tyagi. "Lqr-based ts-fuzzy logic controller design for inverted pendulum-coupled cart system". In: *Systems Thinking Approach for Social Problems: Proceedings of 37th National Systems Conference, December 2013*. Springer. 2015, 207–219. DOI: https://doi.org/10.1007/978-81-322-2141-8_18.

[12] N. S. Bhangal, (2013) *"Design and performance of LQR and LQR based fuzzy controller for double inverted pendulum system"* **Journal of Image and Graphics *1***(3): 143–146. DOI: 10.12720/joig.1.3.143-146.

[13] S. Zhang, R. Liu, X. Qian, et al., (2020) *"Control of a Flexible Manipulator System with Finite-Time Disturbance Observer"* **Journal of Applied Science and Engineering *23***(2): 271–278. DOI: https://doi.org/10.6180/jase.202006_23(2).0011.

[14] N. J. Mathew, K. K. Rao, and N. Sivakumaran, (2013) *"Swing up and stabilization control of a rotary inverted pendulum"* **IFAC Proceedings Volumes *46***(32): 654–659. DOI: https://doi.org/10.3182/20131218-3-IN-2045.00128.

[15] H. O. Wang and K. Tanaka. *Fuzzy control systems design and analysis: a linear matrix inequality approach*. John Wiley & Sons, 2004.

[16] J. Liu, X. Wang, J. Liu, and X. Wang. *Advanced sliding mode control*. Springer, 2011.

[17] X. Wang, Z. Chen, and G. Yang, (2007) *"Finite-time-convergent differentiator based on singular perturbation technique"* **IEEE Transactions on Automatic Control *52***(9): 1731–1737. DOI: 10.1109/TAC.2007.904290.

[18] B. Wenyan, C. Sen, C. HUANG, L. Kunfeng, and H. ZHONG. "A new design of extended state observer for a class of uncertain nonlinear systems with sampled-data measurement". In: *2020 Chinese Automation Congress (CAC)*. IEEE. 2020, 7538–7543. DOI: 10.1109/CAC51589.2020.9326733.